Poly(thiophene)s Prepared via Electrochemical Solid-State Oxidative Cross-Linking. A Comparative Study

Sung-Yeon Jang and Gregory A. Sotzing*

Department of Chemistry and the Polymer Program, Institute of Materials Science, University of Connecticut, 97 N. Eagleville Rd., Storrs, Connecticut 06269

Manuel Marquez

Kraft Foods R&D, The Nanotechnology Lab, 801 Waukegan Rd, Glenview, Illinois 60025, and Los Alamos National Laboratory, Chemical Science & Technology Division, Los Alamos, New Mexico 87545

Received March 26, 2004; Revised Manuscript Received April 12, 2004

ABSTRACT: A comparative study of solid-state oxidative cross-linking (SOC) of polynorbornylenes containing thiophene (**N1T**), bithiophene (**N2T**), and terthiophene pendants (**N3T**) probing polymerization ability, kinetics, and the electrochemical and optical properties of the resulting conductive polythiophene interpenetrating networks (IPN)s is reported. Generally, conductive IPNs prepared from these systems were found to exhibit the capability to shuttle ions with predominant anion transport during the doping/dedoping process and were found to have doping levels ranging from 17 to 36%. **N2T** was found to produce conductive IPNs via SOC with a lower energy π to π^* transition compared to those prepared from **N3T**.

Introduction

Among the variety of intrinsically conducting polymers (ICPs), poly(thiophene)s (**PTs**) have received much attention due to their electronic and optical properties, environmental stability, structural versatility, high conductivity, and potential commercial applicability.[1−4] Potential applications of poly(thiophene)s include their use in organic light-emitting diodes (OLED),[5−8] nonlinear optics,[9] electrochromic windows,[10] energy storage batteries,[11] volatile organic gas sensors,[12,13] and as charge dissipating films.[14] PTs are typically polymerized via oxidative chemical or electrochemical methods from their solutions of monomers, yielding insoluble conducting polymers. Despite their favorable properties, lack of processablity has been a large problem for their application. Alkyl substitution, first reported by Elsenbaumer and co-workers,[15,16] has been the most commonly used method to obtain organic soluble polythiophenes. The synthesis of poly(3-alkylthiophene)s was revolutionized by McCullough and co-workers and by Rieke and co-workers through their achievement of attaining almost exclusive head-to-tail coupling.[17,18] In recent years, water-dispersed poly(3,4-ethylenedioxythiophene)−poly(styrenesulfonate), PEDOT/PSS (Baytron-P),[19−21] has emerged as a commercial success. In general, electrochemical polymerization to produce conductive polymers, although popular for academic study, has several limitations in that the synthesis of conductive polymer from monomer electrolyte solution is low yielding, involves a nucleation and growth mechanism, lacks processability, and quite often results in a grainy morphology.[22−26]

Recently, we have reported a new method to increase yield, processability, and film smoothness of polythiophene via an oxidative electrochemical polymerization procedure not involving a nucleation and growth mechanism, which we have named "solid-state oxidative cross-linking (SOC)".[27] In this technique, a precursor polymer containing covalently bound pendant heterocycles is processed from solution into thin insulating films. The films are then immersed into electrolyte solution by which the polymer swells but does not dissolve. Upon application of an anodic potential, the heterocycles couple to form a conductive interpenetrating network (IPN). The polymer obtained after SOC was shown to retain surface smoothness and shape through the cross-linking process with surface roughness as low as 1 nm.[28] This technology has direct implications toward patterning conductive polymers and developing multilayered devices such as OLEDs and electrochromic devices that require compatibility of processing between layers. Thus, the cross-linked conductive IPN prepared by SOC would have processing compatibility with either a water soluble or organic soluble overlayer.

Herein, we compare the SOC of a polynorbornylene containing thiophene pendants, a polynorbornylene containing bithiophene pendants, and a polynorbornylene containing terthiophene pendants in order to probe polymerization ability, kinetics, and electrochemical and optical properties of the resulting conductive polythiophene IPNs. Furthermore, the electrochemical quartz crystal microbalance (EQCM) was used to establish doping levels and ion transport dominancy upon redox switching. Ion transport is a fundamental property of conjugated polymers that has to be examined for doping and dedoping (charge/discharge cycles) in order to assess the potential utility of these conjugated polymers in applications such as polymeric batteries, capacitors, electrochromic devices, and drug delivery.

Results

Synthesis. The synthesis of thiophene and oligothiophene-derivatized norbornylene monomers and their subsequent polymerization are shown in Scheme 1. **N1T** and **N2T** were prepared by reacting 5-norbornene-2-endo,3-endo-dimethanol with 3-thiophene acetic acid and (2,2′-bithiophene)-3-acetic acid, respectively. **N3T**

* Corresponding author: e-mail Sotzing@mail.ims.uconn.edu.

10.1021/ma049404s CCC: $27.50
Published on Web 05/14/2004

Scheme 1. Thiophene-Based Monomers and Polymers Used in the Study

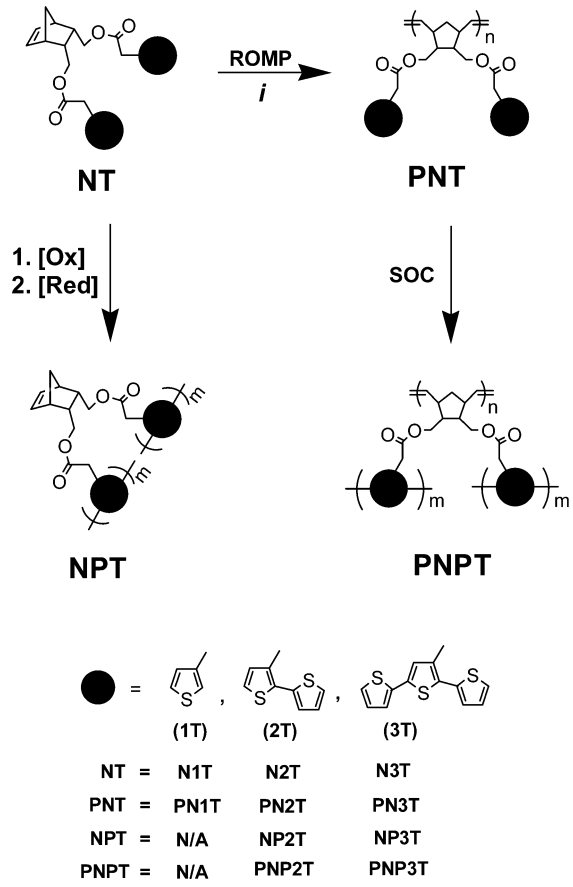

Table 1. Polymerization Yield, Number-Average Molecular Weight, and Polydispersity Index (PDI) of Precursor Polymers PN1T, PN2T, and PN3T

	yield (%)	M_n (g/mol)	PDI
PN1T	74	64 500	1.29
PN2T	85	26 400	1.14
PN3T	75	29 300	1.08

was prepared in accordance to literature procedure.[27] The prepolymers, **PN1T**, **PN2T**, and **PN3T**, were prepared from **N1T, N2T**, and **N3T**, respectively, via ring-opening metathesis polymerization (ROMP) using Grubb's alkylidene catalyst (Scheme 1) in which termination was induced by ethyl vinyl ether. Polymerizations were carried out at room temperature, and as evidenced by ^{1}H and ^{13}C NMR spectroscopy, the thiophene moieties were found to remain intact. The polymerization yield, number-average molecular weight, and polydispersity index (PDI) as derived from gel permeation chromatography (GPC) for **PN1T**, **PN2T**, and **PN3T** are listed in Table 1. **PN1T**, **PN2T**, and **PN3T** are easily soluble in many common organic solvents such as chloroform, tetrahydrofuran, acetone, and toluene. In acetonitrile, which is the solvent in our electrochemical study, the polymers swell to the amount of ca. 8 vol % for **PN3T** and ca. 10 vol % for **PN2T**.

Conventional Electrochemical Polymerization of NT Monomers and Properties of the Resulting Conductive Polymers. Here we define "conventional electrochemical polymerization" as the method by which the monomer is dissolved in electrolyte solution and a potential (or current) is applied to the working electrode by which oxidation of the monomer takes place to form the corresponding radical cation, which then undergoes

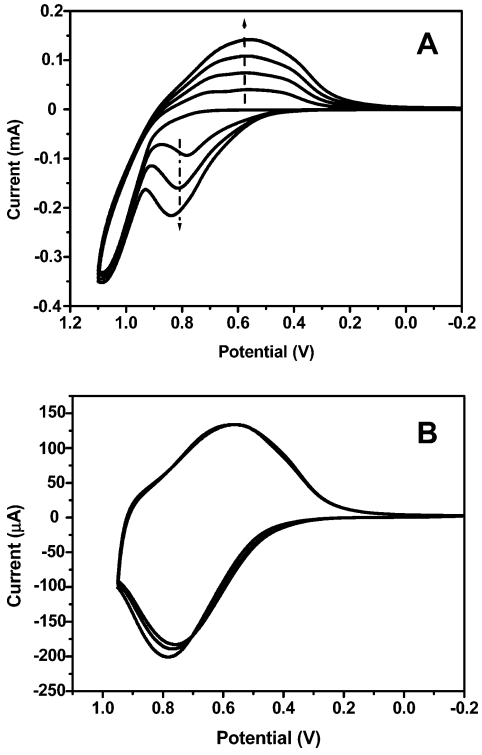

Figure 1. Oxidative electrochemical polymerization of **N2T** at a scan rate of 100 mV/s (A) and the cyclic voltammetry of the resulting polymer **NP2T** (B) at 100 mV/s in 0.1 M TBAP/ACN electrolyte solution using a Pt button working electrode. Potentials reported vs Ag/Ag$^+$ nonaqueous reference electrode (0.455 V vs NHE).

a series of coupling processes to form higher oligomers; after a suitable length of oligomer has been achieved by which the oligomers or polymers become insoluble in solution, electrodeposition takes place via a nucleation and growth mechanism. The conventional electrochemical polymerization of the monomers, **N1T** and **N2T**, was attempted from their 10 mM solution in 0.1 M TBAP/ACN via cyclic voltammetry. Electrochemical polymerization of **N1T** was not successful. This was not surprising considering a structurally similar monomer previously reported by Watson et al. did not polymerize.[29] Figure 1A depicts the formation of **NP2T** from a solution of 10 mM **N2T** in 0.1 M TBAP/ACN. The potential was scanned anodically starting from −0.2 V at a rate of 100 mV/s. At 0.81 V vs Ag/Ag$^+$ nonaqueous reference electrode, there is an onset for oxidation of bithiophene to bithiophene radical cation with an oxidative diffusion-limited peak current at 1.1 V. At a potential above 0.81 V, polymerization takes place as observed by precipitation of a deep blue solid of **NP2T** on the working electrode surface. Upon cathodic scanning, a peak current at 0.56 V occurs that is attributed to the reduction of oxidized **NP2T** to neutral **NP2T**. A second anodic scan reveals an onset for an oxidation at 0.51 V attributed to that for **NP2T**. Since this oxidation occurs at a lower potential than the monomer, it can be concluded that **NP2T** is more highly conjugated than the starting monomer, **N2T**. Increase of cathodic current at 0.56 V and anodic current at 0.81 V as a function of scan cycle indicates more electroactive species on the electrode surface, meaning that additional polymerization of **N2T** occurs.

After polymerization of **N2T**, the electrode coated with a polymer of general structure **NP2T** was washed with acetonitrile and placed into a monomer-free solution of

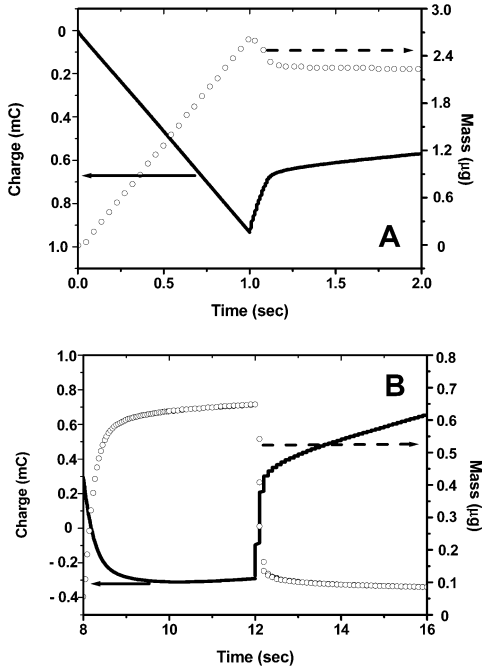

Figure 2. Chronocoulometry and concurrent chronogravimetry during a two-step constant potential polymerization of **N3T** (A) and constant potential redox switch of **NP3T** (B) in TBAP/CH_3CN.

0.1 M TBAP/ACN in order to isolate the electrochemical processes. Figure 1B shows the cyclic voltammogram obtained for **NP2T** at a scan rate of 100 mV/s. As indicated by Figure 1B, the half-wave redox potential of the polymer is 0.56 V.

The electrochemical polymerization, ion transport, and doping of the resulting conductive polymers were studied using the electrochemical quartz crystal microbalance (EQCM). Figure 2A shows the chronocoulometry and concurrent chronogravimetry obtained for the constant potential electrochemical polymerization of **N3T** in 0.1 M TBAP/ACN. Upon application of 0.9 V, the mass increases due to positively charged **NP3T** deposition in addition to the mass of the associated perchlorate counterions. At the end of 1 s the potential is changed to 0 V, at which the polymer is reduced to the neutral form, and a loss of mass on the crystal occurs due to a predominant transport of anions out of the polymer. The percent anions transported during the reduction was calculated from

$$M_{\text{final}} = M_{\text{initial}} - X_{\text{an}}M_{\text{an}} + (Q/F - X_{\text{an}})M_{\text{cat}} \quad (1)$$

where M_{initial} and M_{final} represent the mass of the polymer, **NP3T**, deposited in the oxidized state at the end of the initial one second period and the mass of the neutral polymer after reduction, respectively.[30] M_{an} and M_{cat} are the molar mass of the anion (ClO_4^- ion) and cation (Bu_4N^+ ion), respectively, Q is the charge passed during reduction, F is Faraday's constant, and X_{an} is the number of moles of anion transported. The doping/dedoping behavior of **NP3T** was studied by stepping the potential between 0.9 and 0 V in 4 s pulses (>10 times), as shown in Figure 2B. The ion transport into and out of the film upon oxidation and reduction was found to be 97% anion dominant and the doping level, calculated as the ratio of moles of holes to the moles of thiophene repeat unit, was found to be 35%. Similar ion transport behaviors were observed during electrochemical polymerization for **N2T** and redox switching of the resulting **NP2T** as well.

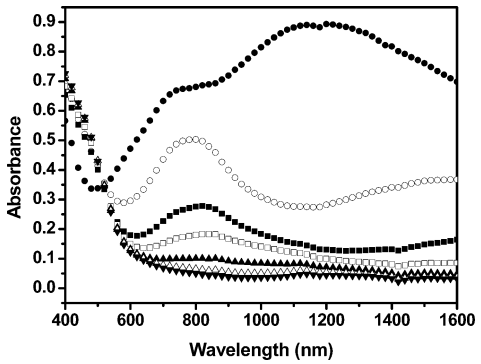

Figure 3. UV−vis−NIR spectra of **NP2T** on chemical reduction: (●) fully oxidized, (○) 1 drop, (■) 2 drops, (□) 3 drops, (▲) 4 drops, (△) 5 drops, and (▼) and fully reduced after dipping the film into acetonitrile containing 5 mM hydrazine.

Optical properties of **NP2T** prepared via conventional electropolymerization were also studied. Figure 3 shows the UV−vis−NIR spectra of **NP2T** upon chemical reduction using 5 mM hydrazine in ACN. First, the UV−vis−NIR spectrum of a fully oxidized **NP2T** film on ITO-coated glass was obtained via application of 1.0 V. An absorption peak at 1200 nm attributed to the π to bipolaron transition resulted. The oxidized **NP2T** was then sequentially reduced by dropwise addition of 5 mM hydrazine/ACN into the ACN solution containing the **NP2T** film. Upon addition of 9 mg of a 5 mM hydrazine solution, the absorption at 1200 nm was significantly reduced, and a new peak at 800 nm, attributed to the higher energy π to bipolaron transition, appeared. Upon further dropwise addition of hydrazine solution, the peak at 1200 nm disappeared, while the absorption at 400 nm, attributed to the π to π^* transition of polythiophene, became more apparent. After addition of 45 mg of 5 mM hydrazine in ACN, **NP2T** was fully reduced, having a single absorption at ∼400 nm and an onset for the π to π^* transition at 605 nm (2.05 eV).

Electrochemical Solid-State Oxidative Cross-Linking (SOC). The electrochemical SOC of **PN1T** and **PN2T** was attempted in 0.1 M TBAP/CH_3CN electrolyte solution. The SOC of **PN3T** was previously reported by our group.[27,28] Figure 4A shows the electrochemical SOC of **PN2T** performed using cyclic voltammetry. The precursor polymer, **PN2T**, was coated from 1 wt % solution in $CHCl_3$ onto the Pt working electrode and then placed in 0.1 M TBAP/ACN. It should be noted that **PN2T** was not soluble in the electrolyte solution, and the insolubility was confirmed by taking UV−vis spectra of the solution containing a film of **PN2T** after a period of 1 h. During the SOC, the only electrochemically polymerizable monomers present are the pendant bithiophenes attached to **PN2T**, which are confined to the surface of the electrode. The cross-linking experiment was initiated at a potential of −0.2 V and scanned in the anodic direction at a scan rate of 50 mV/s. As shown in Figure 4A, at a potential of 0.81 V there is an onset for oxidation that results in a peak at a potential of 1.00 V. Upon cathodic scanning, a reduction peak is observed at a potential of ca. 0.67 V, which can be attributed to the reduction of conductive polythiophene. Upon a second excursion in the anodic direction, there is an onset for oxidation that occurs at approximately 0.31 V, which can be attributed to the oxidation of conjugated polythiophene cross-link units within **PNP2T**.

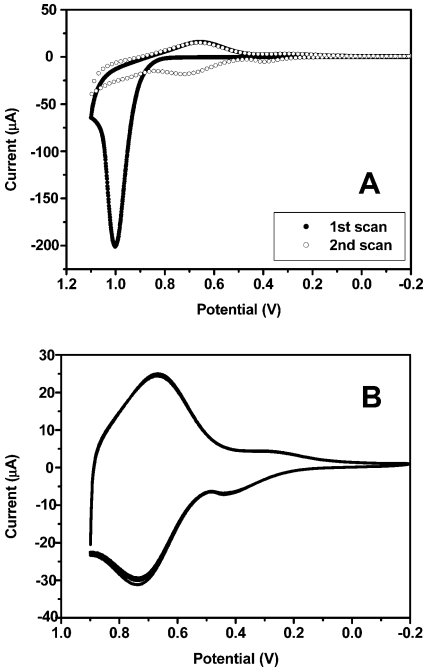

Figure 4. Solid-state oxidative electrochemical cross-linking (SOC) of **PN2T** at a scan rate of 50 mV/s (A) and the cyclic voltammetry of the cross-linked polymer **PNP2T** (B) at 50 mV/s in 0.1 M TBAP/ACN electrolyte solution using a Pt button working electrode. Potentials reported vs Ag/Ag^+ non-aqueous reference electrode (0.455 V vs NHE).

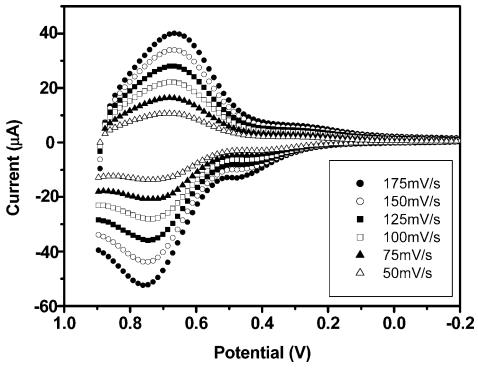

Figure 5. Scan rate dependency study of **PNP2T** at scan rates of 50, 75, 100, 125, 150, and 175 mV/s in 0.1 M TBAP/ACN electrolyte solution. Potentials reported vs Ag/Ag^+ non-aqueous reference electrode (0.455 V vs NHE): (△) 50, (▲) 75, (□) 100, (■) 125, (○) 150, and (●)175 mV/s.

Further scanning in the anodic direction shows a significant reduction in the anodic current response at 1.00 V, indicating most of the bithiophene units were consumed. Scanning in the reverse direction produces a cathodic process with a current response equivalent to that of the first scan, indicating no more formation of conjugated polymer. Thus, oxidative coupling to produce conjugated and conductive polymer was complete upon the first oxidative cycle. It is evident from color observation of the polymer that coupling had taken place since the initially transparent film of **PN2T** turned dark blue upon excursion above 0.82 V.

Figure 4B shows the cyclic voltammetry of **PNP2T** obtained after the solid-state cross-linking of **PN2T**. It should be noted that the oxidation peak of **PNP2T** occurs at 0.64 V and the reduction peak occurs at ca. 0.67 V. Figure 5 shows the current response of **PNP2T** as a function of the scan rate at 50, 75, 100, 125, 150, and 175 mV/s. The linear increase of peak current with respect to the scan rate indicates that the polymer is adhered to the electrode surface. The SOC of **PN1T** performed under identical conditions to **PN2T** was not successful possibly due to overoxidation of the polythiophene that formed. This was apparent in the cyclic voltammetry in that there was an irreversible oxidation of thiophene without a subsequent reduction being apparent.

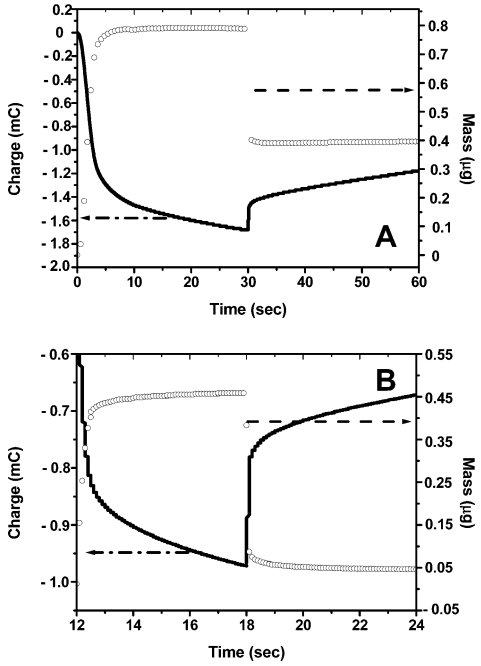

Figure 6. Chronocoulometry and concurrent chronogravimetry during a two-step constant potential solid-state cross-linking of **PN3T** (A) and constant potential redox switch of **PNP3T** (B) in $TBAP/CH_3CN$.

Figure 6A is the chronocoulometry and concurrent chronogravimetry for constant potential electrochemical SOC of **PN3T**. The **PN3T** was coated onto the gold-key electrode (ca. 2.00 μg as measured by QCM) and placed in the EQCM cell filled with 0.1 M TBAP/ACN solution. SOC of **PN3T** was performed at a constant potential of 0.9 V (vs Ag/Ag^+), the oxidation peak potential for **PN3T**. After 30 s, 0.0 V was applied. Each step of oxidation and reduction was 30 s, which was sufficient to give enough time to reach equilibrium of ion movement. As soon as the potential (0.9 V) was applied, oxidative cross-linking of **PN3T** is initiated, taking anions into the polymer matrix to compensate positive charges developed on the terthiophene pendant units. As a result, the mass of polymer increases while the counterions are moving in; however, it reaches a steady state after ca. 3 s, indicating consumption of terthiophene units is completed. In other words, the cross-linking reaction is finished within 3 s. During this time, a mass increase of 781 ng was observed mainly due to the incorporation of anion to compensate positive charges attributed to the oxidation of terthiophene units and its resulting conducting polymer **PNP3T**. Upon switching to −0.2 V, the potential that **PNP3T** is reduced, the mass dropped drastically in less than a second and then maintained a steady mass. This indicates that the shuttling of anions happened instantaneously while polymer was reduced. During this dedoping, 389 ng of mass was decreased as a result of ion shuttling, which is a combination of anion migration out of the polymer film and cation incorporation in to the polymer film. The

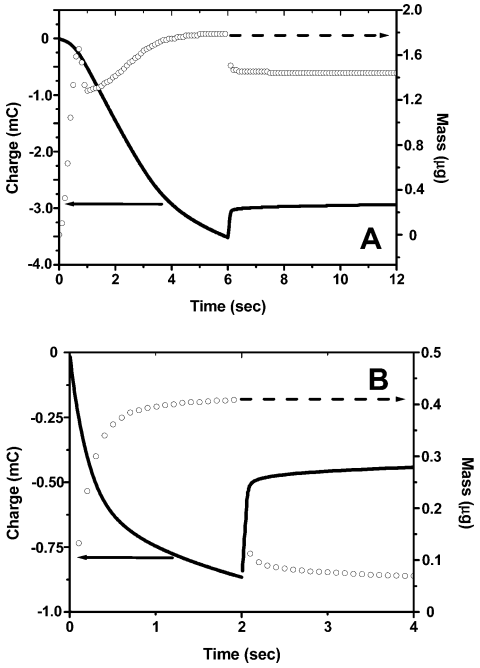

Figure 7. Chronocoulometry and concurrent chronogravimetry during a two-step constant potential solid-state cross-linking of **PN2T** (A) and constant potential redox switch of **PNP2T** (B) in TBAP/CH_3CN.

ratio of anion and cation which transport during the solid-state oxidative cross-linking was calculated to be 92:8, a high anion dominancy, according to the eq 1. The doping/dedoping behavior of **PNP3T** was also studied by stepping the potential between 0.9 and −0.2 V with a pulse width of 6 s (>10 times). The results are shown in Figure 6B. **PNP3T** switches nicely; the ion transport ratio was calculated to be similar to the anion dominancy (89%), and the doping level calculated as the ratio of moles of electrons to the moles of thiophene repeat units deposited on the electrode was found to be 36%.

Figure 7A shows the charge and mass change during electrochemical SOC of **PN2T** via applying constant potential. 3.57 μg of **PN2T**, coated onto a gold-key electrode, was placed in the EQCM cell filled with 0.1 M TBAP/CH_3CN solution. Cross-linking of **PN2T** to **PNP2T** was performed by applying a constant potential of 1.0 V (vs Ag/Ag^+), the peak potential of the oxidation of **PN2T** (Figure 7A), for 6 s followed by reduction of the cross-linked conductive polymer at −0.2 V for 6 s. The percent ratio of anion to cation transported during the solid-state oxidative cross-linking was calculated to be 89% anion dominancy according to eq 1. The doping/dedoping behavior of **PNP2T** was also studied by stepping the potential between 0.9 and −0.2 V in 6 s pulses (>10 times). The results are shown in Figure 7B. The ion transport ratio was calculated as having similar anion dominancy (93%), and the doping level calculated as the ratio of moles of holes to the moles of thiophene repeat units deposited on the electrode was found to be 17%.

Optical properties of **PNP2T** were obtained using UV−vis−NIR spectroscopy by sequentially reducing a **PNP2T** film chemically (Figure 8). The **PN2T** film spin-coated on ITO-coated glass was converted to **PNP2T** via electrochemical SOC by cyclic voltammetry. The resulting **PNP2T** film in the oxidized state was sequentially reduced with 5 mM hydrazine in ACN. The spectrum in the fully oxidized state exhibits two peaks

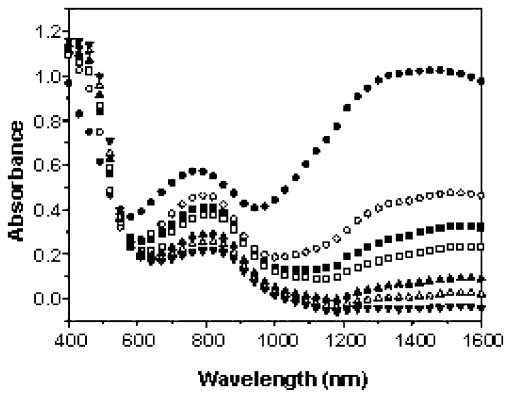

Figure 8. UV−vis−NIR spectra of **PNP2T** on chemical reduction: (■) fully oxidized, (□) 1 drop, (●) 2 drops, (○) 4 drops, (▲) 6 drops, (△) 8 drops, and (▼) after dipping the film into acetonitrile containing 5 mM hydrazine.

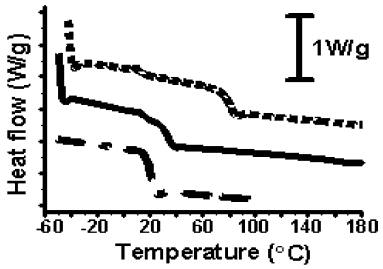

Figure 9. Differential scanning calorimetery (DSC) analysis of **PN1T** (− ·), **PN2T** (—), and **PN3T** (· · ·).

at 780 nm (1.59 eV) and 1510 nm (0.82 eV), which can be attributed to the transitions from the valence band to the first and second bipolaron bands. Upon dropwise addition of chemical reducing agent (5 mM hydrazine in ACN), the polymer is sequentially reduced, upon which there is a reduction in the absorbance for the valence to bipolaron transitions and an increase in absorbance for the valence to conduction band transition. **PNP2T** exhibits a band gap of ca. 2.10 eV (588 nm) with a peak at 2.79 eV (445 nm) in fully reduced state. **PNP2T** prepared using ferric chloride was found to have a conductivity of 1.2×10^{-3} S/cm.

Thermal Analysis. The glass transition temperatures (T_g) of the three precursor polymers, **PN1T**, **PN2T**, and **PN3T**, were studied using differential scanning calorimetery (DSC). Figure 9 shows the DSC results of these three precursor polymers. The samples were heated to 100 °C and immediately quenched using liquid nitrogen until they reach −50 °C, and then DSC analysis was performed by heating at the scan rate of 10 °C/min. As shown in Figure 9, the T_g of **PN1T**, **PN2T**, and **PN3T** was 21, 34, and 80 °C, respectively. As more aromatic portions are attached to the flexible polynorbornene backbone, the glass transition temperature of the precursor polymer increases. There were no observable melting temperatures indicating these precursor polymers are highly amorphous. Thermal stability of the precursor polymers was also studied using thermal gravimetric analysis (TGA). Figure 10 shows the TGA results of **PN3T** and **PNP3T**. Thermal stability of the precursor polymer (**PN3T**) was significantly increased via SOC, especially in the high-temperature regime. The temperatures of 5% weight loss of **PN3T** and **PNP3T** were 293 and 332 °C, and those of 50% weight loss were 355 and 507 °C, respectively.

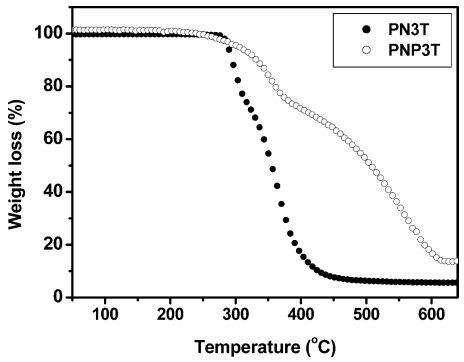

Figure 10. Thermal gravimetric analysis (TGA) of **PN3T** and **PNP3T** at a scan rate of 20 °C/min.

Discussion

In our previous work,[27] a conducting polymer was prepared using solid-state oxidative cross-linking (SOC), and the electrochemical, optical, and electronic properties of the polymer were similar to that of conducting polymer prepared by conventional electrochemical polymerization. In this paper, three different thiophene-based monomers, **N1T**, **N2T**, and **N3T**, in which the thiophene (**T**), bithiophene (**2T**), and terthiophene (**3T**) groups are attached into a norbornene molecule, were studied. All three thiophene-based electroactive units have different oxidation potentials, which dictate polymerization conditions. The thiophene-based system **N1T** was not polymerized to conducting polymers either by electroprecipitaion from monomer solution or by electrochemical SOC from its precursor polymer **PN1T**. Electrochemical polymerizations of ester-substituted thiophenes in other reports were also not successful,[29,31] and SOC of **PN1T** was also not achievable due to the same reason. The bithiophene-based system **N2T** was nicely polymerized via both the conventional electroprecipitation method and electrochemical SOC from its precursor polymer **PN2T**. The lower oxidation potential of the ester-linked bithiophene group allowed facile polymerization to the polythiophenes. Onset oxidation potentials of **N2T** and **PN2T** were identical attributed to oxidation of bithiophene units in **N2T** and **PN2T**, and the positions of peak oxidation potentials were slightly different due to their different polymerization mechanisms, while the former is due to diffusion limitation of monomer molecules from a solution and the latter comes from the consumption rate of pendant groups. The peak breadth in SOC of **PN2T** was narrower than that of electroprecipitation of **N2T** because there is no additional supplying of electroactive units, bithophenes, which are diffusing near the electrode during the polymerization process in the case of conventional electroprecipitation of **N2T**. The ion transport behavior of polythiophenes both from the terthiophene system, **NP3T** and **PNP3T**, and the bithiophene system, **NP2T** and **PNP2T**, show typical ion transport behavior of polythiophene. Ion transport behavior of all four conducting polymers in a given electrolyte system (TBAP/ACN) was highly anion dominant, and the doping levels of those systems show from ca. 1 charge/3 thiophene rings to ca. 1 charge/6 thiophene rings, which is the typical range of 3-substituted poly(thiophenes), which is 1 charge /12 thiophene rings to 1 charge/3 thiophene rings.[1,25] Ion transport behavior of polythiophenes prepared via the conventional electroprecipitaton method and the SOC method were very similar regardless of the bi- and terthiophene system, although the former method is precipitation and the latter is cross-linking in a confined polymeric matrix.

The optical properties of the resulting polythiophene from the bithiophene system shows the same trend with that of the polythiophene from the terthiophene system we reported earlier.[27,28] The polythiophene prepared via SOC, **PNP2T**, shows λ_{max} at 445 nm, whereas PT prepared via conventional electroprecipitation, **NP2T,** shows λ_{max} lower than 400 nm. Similarly, **PNP3T** shows λ_{max} at 440 nm whereas **NP3T** at 400 nm in their reduced forms. This higher conjugation length in the solid-state cross-linking system compared to the solution precipitation system could be attributed to the different mechanism of the two systems. In the electroprecipitation process, the polythiophene from the coupling of monomeric thiophene units precipitate onto an electrode surface in early stage depending on their solubility in electrolyte solution before they reach the maximum conjugation length. However, for SOC, the polythiophene is covalently tethered on the main chain backbone, polynorbornene; therefore, the coupling reaction is more governed by chain mobility than solubility in electrolyte solution. From our observation, it seems that the premature precipitation of polythiophene tends to result in shorter conjugation than the polythiophene from SOC. This tells us that the solid-state cross-linking process in polymer matrix is more efficient than the conventional electroprecipitation process in terms of coupling reaction between electroactive thiophene units. Furthermore, conjugation lengths of polythiophenes were quite consistent with other reports of substituted polythiophenes.[32−34] Polythiophene prepared from the higher oligomer units has a shorter conjugation length based on our UV−vis absorption spectra results, just as in other reports, which has been attributed to the lower reactivity of the monomer.[32−34] The onset band-edge gap of the two polymers prepared via solid-state cross-linking, **PNP2T** and **PNP3T**, was 588 nm (2.13 eV) and 600 nm (2.08 eV), respectively, which are typical numbers for polythiophenes.

The glass transition temperatures of the three prepolymers increased as the size of the pendant heterocycles increased as measured by DSC, and in the case of **PNP2T**, the glass transition temperature was shifted to a higher temperature than that of **PN2T** due to the reduction of free volume via SOC. The thermal stability of **PNP3T** was higher than that of **PN3T**, indicating the formation of a network structure via SOC increases the thermal stability of polymer.

Conclusion

A comparative study of polythiophenes of three different 3-substituted thiophene systems, which have different oxidation potentials, was demonstrated via conventional electroprecipitation and solid-state oxidative cross-linking (SOC). The thiophene-based monomer, **N1T**, was not polymerized by either method due to the high oxidation potential; however, the bi- and terthiophene systems, **N2T** and **N3T**, were polymerized by both techniques, and the SOC technique tends to result in longer conjugation length than that of conventional electroprecipitation. Correspondent to other reports,[32−34] polythiophenes from higher oligomeric units give a lower degree of conjugation than that of lower oligomeric units in both electroprecipitation and solid-state cross-linking.

Ion transport behavior of polythiophenes prepared by the two different methods, electroprecipitation and SOC,

was also studied. Generally, ion transport behavior and doping level in polythiophene from the SOC system showed behavior similar to that of PT from electroprecipitation. The doping level of **PNP3T** was 36% (1 charge every 3 thiophene rings) and **PNP2T** was 17% (1 charge every 6 thiophene rings), a typical range for 3-substituted poly(thiophene)s in other reports. All of these results indicate that conductive polymer IPNs could be used for applications that conductive polymers prepared via conventional electrochemical polymerization are presently being used.

Experimental Section

Chemicals. 3-Thiopheneacetic acid, 5-norbornene-2-endo,3-endo-dimethanol, ethyl thiophene-3-acetate, 2-(tributylstannyl)thiophene, dichlorobis(triphenylphosphine)palladium, deuterated chloroform ($CDCl_3$), and *p*-toluenesulfonic acid were purchased from Aldrich Chemical Co. and used as received. Grubb's alkylidene catalyst and iron(III) chloride were purchased from Strem Chemicals, Inc., and used without further purification. Tetrahydrofuran (THF) and toluene were distilled over sodium and benzophenone under nitrogen, and methylene chloride (CH_2Cl_2) and acetonitrile (CH_3CN) were distilled over calcium hydride (CaH_2) under nitrogen before use. *N*-Bromosuccinimide (NBS), Acros, was recrystallized from deionized water and vacuum-dried. Tetrabutylammonium perchlorate (TBAP) was prepared via addition of 70% perchloric acid solution purchased from Fisher Scientific to an aqueous solution of tetrabutylammonium bromide (TBABr) purchased from ACROS Organics. TBAP was recrystallized from ethanol before use. Silica gel was purchased from SAI, and their particle size was between 32 and 63 μm. **Warning:** *Perchloric acid and organic perchlorates can be explosive when heated. Furthermore, being a strong oxidizing acid, perchloric acid should never be stored or mixed with organics. Proper safety and storage procedures should be excercised when handling both perchloric acid and organic perchorate salts.* Hydrazine monohydrate was used as received from Strem Chemicals, Inc., and ACROS Organics, respectively. 5-Norbornene-endo-2,3-bis(methylene-3′-[2,2′:5′,2″]-terthiophene acetate) (**N3T**) and **PN3T** were prepared in accordance to literature procedures.[27]

Instrumentation. ^{1}H and ^{13}C nuclear magnetic resonance (NMR) spectra were recorded using a Bruker 400 FT-NMR spectrometer. ^{1}H NMR data are reported as follows: chemical shift (multiplicity: b = broad signal, s = singlet, d = doublet, t = triplet, q = quartet, dd = doublet of doublets, and m = multiplet, integration). ^{1}H and ^{13}C chemical shifts are reported in ppm downfield from tetramethylsilane (TMS) reference using residual protonated solvent resonance as an internal standard. Number-average molecular weight and polydispersity index (PDI) were obtained using monodisperse polystyrene standards and a Waters 150-C plus gel permeation chromatograph (GPC) equipped with UV/vis, refractive index, and evaporative light scattering detectors. Thermal analysis was performed using TA Instrument DSC 2920 and Hi-Res TGA 2950 for differential scanning calorimetery (DSC) and thermal gravimetric analysis (TGA).

5-Norbornene-endo-2,3-bis(methylenethiophene acetate), N1T. To a 250 mL three-neck round-bottom flask that had been vacuum-dried and nitrogen purged and fitted with a Dean-Stark trap was added 1.46 g (9.5 mmol) of 5-norbornene-2-endo,3-endo-dimethanol. 120 mL of toluene was added under nitrogen, followed by the addition of 2.84 g (20 mmol) of 3-thiopheneacetic acid and 160 mg of *p*-toluenesulfonic acid. The three solids were completely dissolved after 10 min, and the solution was refluxed for 6 h while the bottom layer in the Dean-Stark trap was collected (80 mL total). The reaction mixture was cooled to room temperature, washed with water (50 mL), and extracted with ether (3 × 50 mL). The organic portion was separated and washed with brine, dried over anhydrous sodium sulfate, and filtered, and then the solvent was removed under vacuum. The resulting yellow oil was dissolved in 5 mL of CH_2Cl_2, and column chromatography was performed using silica gel with CH_2Cl_2/MeOH (98:2) as the eluent to yield 2.90 g (75%) of the desired product as light yellow oil. ^{1}H NMR ($CDCl_3$): 7.26 (dd, 2H), 7.14 (d, 2H), 7.04 (dd, 2H), 6.10 (s, 2H), 3.90 (dd, 2H), 3.78 (s, 2H), 3.63 (s, 4H), 2.82 (s, 2H), 2.49 (m, 2H), 1.48 (d, 1H), 1.29 (d, 1H). ^{13}C NMR ($CDCl_3$): 36.30, 40.83, 45.75, 49.32, 65.33, 123.19, 126.10, 126.20, 128.77, 133.90, 135.71, 171.24. FTIR: 3100 and 3040 cm^{-1} (aromatic and vinyl C−H stretching), 2967 and 2873 cm^{-1} (aliphatic C−H stretching), 1734 cm^{-1} (ester C═O stretching), 1259 cm^{-1} (ester C−C−O stretching).

Ethyl 2-Bromothiophene-3-acetate. In a 250 mL three-neck flask containing 50 mL of $CHCl_3$ and 50 mL of glacial acetic acid, 9.5 g (0.0558 mol) of ethyl thiophene-3-acetate was added, followed by 9.93 g (0.0558 mol) of NBS. The mixture was stirred at room temperature for 12 h. The mixture became clear yellow solution after 1 h and then was cooled to room temperature and poured into 200 mL of deionized (DI) water. The organic portion was washed again with 100 mL of DI water and then finally washed with 100 mL of 5% aqueous sodium bicarbonate solution. After having been dried over magnesium sulfate, the solvent was filtered, and the product was concentrated under vacuum. The resulting residue was vacuum-distilled at 95 °C under 1 mmHg, yielding 12.3 g (88% yield). ^{1}H NMR ($CDCl_3$): 1.26 (t, 3H), 3.60 (s, 2H), 4.16 (q, 2H), 6.93 (d, 1H), 7.22 (d, 1H).

Ethyl (2,2′-Bithiophene)-3-acetate. To a dried 250 mL three-neck round-bottom flask containing 50 mL of dry THF containing dichlorobis(triphenylphosphine)palladium (1.20 g) was cannulated 8.5 g (34 mmol) of ethyl 2-bromothiophene-3-acetate dissolved in 80 mL of dry THF. The mixture was refluxed for 24 h. The solvent was removed under vacuum, and the residue was dissolved in CH_2Cl_2 (100 mL). The solution was washed with water (100 mL × 3) and dried with $MgSO_4$. The solvent was evaporated, and the residue was purified by column chromatography using silica with toluene as eluent. A total of 5.9 g of ethyl(2, 2′-bithiophene)-3-acetate was obtained as a clear oil (69% yield). ^{1}H NMR ($CDCl_3$): 7.33 (dd, 1H), 7.23 (d, 1H), 7.19 (dd, 1H), 7.08 (dd, 1H), 7.05 (d, 1H), 4.17 (q, 2H), 3.75 (s, 2H), 1.27 (t, 3H)

(2,2′-Bithiophene)-3-acetic Acid. In a 500 mL flask, 5.5 g (22 mmol) of ethyl (2,2′-bithiophene)-3-acetate dissolved in 50 mL of methanol was added, followed by 200 mL of 15% aqueous sodium hydroxide solution. The solution was refluxed for 3 h. After cooling the mixture to room temperature, the solution was concentrated via methanol removal using rotary evaporation. The aqueous solution was washed with diethyl ether and then acidified with HCl to pH 1, upon which precipitation occurs. The white precipitate was dissolved in CH_2Cl_2 (150 mL × 3), and the organic portion was collected. Chloroform was removed using a rotary evaporator after drying over magnesium sulfate to yield 4.7 g of white solid, 96% yield. ^{1}H NMR ($CDCl_3$): 7.34 (dd, 1H), 7.25 (d, 1H), 7.18 (dd, 1H), 7.08 (dd, 1H), 7.06 (d, 1H), 3.80 (s, 2H).

5-Norbornene-endo-2,3-bis(methylene-3-[2,2′]-bithiophene acetate), N2T. To a 250 mL three-neck round-bottom flask that had been vacuum-dried and nitrogen-purged and fitted with a Dean-Stark trap was added 2.46 g (11 mmol) of (2,2′-bithiophene)-3-acetic acid, 0.81 g (5.2 mmol) of 5-norbornene-2-endo,3-endo-dimethanol, and 100 mL of toluene under nitrogen, followed by the addition of 84 mg of *p*-toluenesulfonic acid. The three solids completely dissolved after 10 min, and the solution was refluxed for 6 h while the bottom layer in the Dean-Stark trap emptied occasionally (60 mL of solution collected in total). The reaction mixture was cooled to room temperature and washed with water (50 mL), and the product was extracted into ether. The organic portion was separated and washed with brine, dried over sodium sulfate, and filtered, and then the solvent was removed under vacuum. The resulting yellow oil was purified by column chromatography using silica gel and ethyl acetate as the eluent to yield 1.4 g (48% yield) of the desired product as a clear oil. ^{1}H NMR ($CDCl_3$): 7.32 (dd, 2H), 7.22 (d, 2H), 7.18 (dd, 2H), 7.07 (dd, 2H), 7.04 (d, 2H), 6.08 (s, 2H), 3.79 (m, 2H), 3.84 (m, 2H), 3.74 (s, 4H), 2.79 (s, 2H), 2.42 (m, 2H), 1.46 (d, 1H), 1.27 (d, 1H). ^{13}C NMR ($CDCl_3$): 35.34, 40.95, 45.85, 49.42, 53.86,

65.52, 124.92, 126.57, 127.30, 128.11, 130.60, 130.73, 133.73, 135.52, 135.84, 171.11. FTIR: 3100 and 3062 cm^{-1} (aromatic and vinylic C−H stretching); 2967 and 2868 cm^{-1} (aliphatic C−H stretching); 1734 cm^{-1} (ester C═O stretch); 1259 cm^{-1} (ester C−C−O stretching).

Poly[5-norbornene-endo-2,3-bis(methylenethiophene acetate)], PN1T. A solution of **N1T** (1.33 g, 3.30 mmol) in dry CH_2Cl_2 (10 mL) was transferred via cannular into a 100 mL Schlenk flask, previously vacuum-dried and nitrogen-purged, under nitrogen containing 18 mg of Grubb's alkylidene catalyst (0.02 mmol) and 5 mL of CH_2Cl_2. The mixture was allowed to stir for 30 min followed by irreversible termination via the addition of 3 mL of ethyl vinyl ether. The solution was then concentrated under vacuum. The polymer was precipitated three times in pentane (300 mL), filtered, and then dried under vacuum to yield 0.98 g (75%) of gumlike polymer. The number-average molecular weight was determined to be 65 000 g/mol (PDI = 1.28). ^1H NMR ($CDCl_3$): 7.24 (b, 2H), 7.10 (b, 2H), 7.00 (b, 2H), 5.28 (s, 2H), 4.00 (b, 4H), 3.56 (s, 4H), 2.62 (b, 2H), 2.36 (b, 2H), 1.90 (b, 1H), 1.27 (b, 1H).

Poly[5-norbornene-endo-2,3-bis(methylene-3-[2,2′]-bithiophene acetate)], PN2T. **PN2T** was polymerized from **N2T** in a manner similar to **PN1T** with a yield of 94%. The number-average molecular weight was determined to be 26 400 g/mol with PDI of 1.14. ^1H NMR ($CDCl_3$): 7.19 (b, 2H), 7.06 (b, 4H), 6.91 (b, 4H), 5.13 (s, 2H), 3.93 (b, 4H), 3.60 (s, 4H), 2.45 (b, 2H), 2.21 (b, 2H), 1.78 (b, 1H), 1.20 (b, 1H). ^{13}C NMR ($CDCl_3$): 35.16, 44.49, 44.52, 63.68, 124.81, 126.44, 127.10, 128.10, 130.39, 130.60, 133.62, 135.33, 171.00. FTIR: 3105 and 3065 cm^{-1} (aromatic and vinylic C−H stretching); 2954 and 2863 cm^{-1} (aliphatic C−H stretching); 1731 cm^{-1} (ester C═O stretch); 1244 cm^{-1} (ester C−C−O stretching).

General Electrochemistry. All electrochemistry experiments were carried out in a conventional three-electrode cell using a Pt button working electrode of 2 mm diameter, a 1 cm^2 platinum flag counter electrode, and a nonaqueous Ag/0.01 M Ag^+ (silver wire in 0.1 M TBAP in CH_3CN) reference electrode. The reference electrode was calibrated to be 0.456 V vs the standard hydrogen electrode (SHE) using a 20 mM ferrocene standard solution. Solid-state electrochemical polymerization of precursor polymers was carried out in monomer-free 0.1 M TBAP/CH_3CN electrolyte solution, and electrochemical polymerization via the conventional electroprecipitation technique was carried out using a 10 mM concentration of monomer in TBAP/ CH_3CN. Electrochemical characterizations of the conducting polymers onto the button working electrodes were performed in a monomer-free electrolyte solution after washing of the conducting polymers with CH_3CN.

Optoelectrochemistry. A Perkin-Elmer Lambda 900 UV−vis−NIR spectrophotometer was used, and the data were reported using UV winlab software. The polymer **NP2T** was deposited onto an indium-doped tin oxide (ITO)-coated glass working electrode electrochemically from a 10 mM solution of the monomer **N2T** in 0.1 M TBAP/ACN via scanning from 0 to 1.10 V at the scan rate of 0.1 V/s. The UV−vis−NIR spectra were taken upon fully oxidized state and then sequentially reducing the polymer film. The ITO-coated glass had a nominal resistance of 100 ohms with a dimension of 7 mm × 50 mm × 0.7 mm and was purchased from Delta Technologies, Ltd.

UV−Vis−NIR Study upon Sequential Reduction of PNP2T with Hydrazine. 200 nm thick **PN2T** films were obtained on indium tin oxide (ITO)-coated glass from a 1 wt % solution of **PN2T** in chloroform by spin-coating at 1000 rpm and then cross-linked to **PNP2T** by scanning between −0.2 and 1.1 V (vs Ag/Ag^+). This **PNP2T** film was dipped into an acetonitrile solution containing 0.01 M $FeCl_3$ for 3 min until the fully reduced orange colored film turned to the fully oxidized dark blue film. The film was washed with acetonitrile and placed in the acetonitrile. The UV/vis/NIR spectrum of fully oxidized state was obtained, and then sequential reduction was carried out by subsequent adding a drop of 0.005 M hydrazine/acetonitrile solution into the solution which contain a film of **PNP2T**. At each reduction step, the film was allowed to sit in this solution for 5 min before taking the UV−vis−NIR spectrum. This process was then repeated several times. The film was finally dipped into 0.005 M hydrazine/acetonitrile for full reduction.

Electrochemical Quartz Crystal Microbalance (EQCM). The EQCM cell was connected to a CH Instrument 400 potentiostat equipped with oscillator circuit. Polished quartz crystals coated with a 0.201 in. diameter key electrode on both sides and operating at a resonant frequency of 7.995 MHz were purchased from International Crystal Manufacturing. The key electrode comprised of a 1000 Å thick gold coating with a 100 Å chromium underlay was soldered to leads for electrical contact that were sealed away from the solution. A 1 cm^2 platinum flag was used as the counter electrode, and a nonaqueous Ag/Ag^+ (0.456V vs NHE) was used as the reference electrode. All the EQCM studies were carried out using 0.1 M TBAP/CH_3CN electrolyte solution.

SOC of PN2T Using Chemical Oxidant and Conductivity Measurement. A 1 wt % solution of **PN2T** in chloroform was spun-coat at a rate of 1000 rpm onto a glass slide (2.2 cm × 2.2 cm). The resulting film was light yellow with a thickness of 200 nm as measured by an optical profiler. The SOC of **PN2T** was performed by dipping the film into an acetonitrile solution containing 0.01 M $FeCl_3$ for 15 min. Conductivity was measured using a four-point collinear array utilizing a Keithley Instruments 224 constant current source to supply 0.01 μA across the outer leads and measuring the voltage difference between the two inner leads using a Keithley Instruments 2700 multimeter. Resistance was calculated using Ohm's law, and the conductivity was determined in accordance with the equation $\sigma = l/twR$, where σ is the conductivity in units of S/cm, R is the resistance in ohms, l is the distance between the two inner leads in cm, w is the width of the film in cm, and t is the film thickness in cm. It should be noted that the conductivity was performed under normal laboratory conditions at a humidity of ca. 35%.

Acknowledgment. We thank Kraft Foods, Inc. (Nanotek consortium), and the National Science Foundation−CAREER (CHE-0349121) for financial support of this work.

References and Notes

(1) *Handbook of Conducting Polymers*, 2nd ed.; Skotheim, T. A., Elsenbaumer, R. L., Reynolds, L. R., Eds.; Marcel Dekker: New York, 1998.
(2) Groenendaal, L. B.; Jonas, F.; Freitag, D.; Pielartzik, H.; Reynolds, J. R. *Adv. Mater.* **2000**, *12*, 481−494.
(3) McCullough, R. D. *Adv. Mater.* **1998**, *10*, 93−116.
(4) Roncali, J. *Chem. Rev.* **1997**, *97*, 173−206.
(5) Yu, G.; Heeger, A. J. *Synth. Met.* **1997**, *85*, 1183.
(6) Friend, R. H.; Gymer, R. W.; Holmes, A. B.; Burroughes, J. H.; Marks, R. N.; Taliani, C.; Bradley, D. D. C.; Dos Santos, D. A.; Bredas, J. L.; Logdlund, M.; Salaneck, W. R. *Nature (London)* **1999**, *397*, 121−128.
(7) Sirringhaus, H.; Tessler, N.; Friend, R. H. *Science* **1998**, *280*, 1741−1744.
(8) Torsi, L.; Dodabalapur, A.; Rothberg, L. J.; Fung, A. W. P.; Katz, H. E. *Science* **1996**, *272*, 1462−1464.
(9) Ma, H.; Chen, B.; Sassa, T.; Dalton, L. R.; Jen, A. K.-Y. *J. Am. Chem. Soc.* **2001**, *123*, 986−987.
(10) Sapp, S. A.; Sotzing, G. A.; Reynolds, J. R. *Chem. Mater.* **1998**, *10*, 2101−2108.
(11) Ferraris, J. P.; Eissa, M. M.; Brotherston, I. D.; Loveday, D. C. *Chem. Mater.* **1998**, *11*, 3528−3535.
(12) McQuade, D. T.; Pullen, A. E.; Swager, T. M. *Chem. Rev.* **2000**, *100*, 2537−2574.
(13) Sotzing, G. A.; Briglin, S.; Grubbs, R. H.; Lewis, N. S. *Anal. Chem.* **2000**, *72*, 3181.
(14) Lerch, K.; Jonas, F.; Linke, M. *J. Chim. Phys. Phys.-Chim. Biol.* **1998**, *95*, 1506.
(15) Elsenbaumer, R. L.; Jen, K.; Oboodi, R. *Synth. Met.* **1986**, *15*, 169.
(16) Elsenbaumer, R. L.; Miller, G. G. *J. Chem. Soc., Chem. Commun.* **1986**, 1346.
(17) (a) McCullough, R. D.; Lowe, R. D. *J. Chem. Soc., Chem. Commun.* **1992,** *1*, 70−72. (b) McCullough, R. D.; Lowe, R. D.; Jayaraman, M.; Anderson, D. L. *J. Org. Chem.* **1993**, *58*,

904−912. (c) McCullough, R. D.; Tristram-Nagle, S.; Williams, S. P.; Lowe, R. D.; Jayaraman, M. *J. Am. Chem. Soc.* **1993**, *115*, 4910−4911.
(18) Chen, T. A.; Rieke, R. D. *J. Am. Chem. Soc.* **1992**, *114*, 10087−10088.
(19) Bayer AG, Eur. Patent 339340, 1988.
(20) Jonas, F.; Schrader, L. *Synth. Met.* **1991**, *41*−*43*, 831.
(21) Heywang, G.; Jonas, F. *Adv. Mater.* **1992**, *4*, 116.
(22) Sayre, C. N.; Collard, D. M. *Langmuir* **1995**, *11*, 302−306.
(23) Sayre, C. N.; Collard, D. M. *Langmuir* **1997**, *13*, 714−722.
(24) Yassar, A.; Roncali, J.; Garnier, F. *Macromolecules* **1989**, *22*, 804−809.
(25) Sanchez, J. V.; Diaz, R.; Herraste, P.; Ocon, P. *Polym. J.* **2001**, *33*, 514−521.
(26) Valle, M. A.; Cury, P.; Schrebler, R. *Electrochim. Acta* **2002**, *48*, 397−405.
(27) Jang, S.; Sotzing, G. A.; Marquez, M. *Macromolecules* **2002**, *35*, 7293−7300.
(28) Jang, S.; Sotzing, G. A.; Marquez, M. *ACS Symp. Ser.* **2004**, *874*, 44−53.
(29) Watson, K. J.; Wolfe, P. S.; Nguyen, S. T.; Zhu, J.; Mirkin, C. A. *Macromolecules* **2000**, *33*, 4628−4633.
(30) Berlin, A.; Schiavon, G.; Zecchin. S.; Zotti. G *Synth. Met.* **2001**, *119*, 153.
(31) Welzel, H. P.; Kossmehl, G.; Boettcher, H.; Engelmann, G.; Hunnius, W.-D. *Macromolecules* **1997**, *30*, 7419−7426.
(32) Zotti, G.; Marin, R. A.; Gallazzi, M. C. *Chem. Mater.* **1997**, *9*, 2945−2950.
(33) Wei, Y.; Chan, C.; Tian, J.; Jang, G.; Hsueh, K. F. *Chem. Mater.* **1991**, *3*, 888−897.
(34) Zotti, G.; Gallazzi, M. C.; Zerbi, G.; Meille, S. V. *Synth. Met.* **1995**, *73*, 217−225.

MA049404S